

Constraining the Locations of Microlenses Towards the LMC

Mark Yashar¹

ABSTRACT

The MACHO Project microlensing survey has placed important constraints on the fraction of massive compact halo objects (MACHOs; e.g. brown dwarfs, white dwarfs, neutron stars, and black holes) in the Milky Way (MW) halo. However, because the three fundamental microlensing parameters (the mass, distance, and velocity of the lens) are all degenerate in the observed microlensing event duration, the location and nature of the microlenses remains an open question. Additional information on the location of the lenses can be gained by comparing the color-magnitude diagram (CMD) of microlensing source stars to the average population of the Large Magellanic Cloud (LMC) disk. This analysis suggests that the source stars are located in the LMC disk and the lenses are located in the MW halo. Work involving the use of synthetic CMDs will be described as well. Finally, future work regarding a project on dark energy observables will be outlined.

1. Introduction

Recent measurements and analysis of the Cosmic Microwave Background (CMB) [1,2] combined with supernova observations (e.g., [3,4]) have now placed us in an era of "precision cosmology" in which the basic composition of the universe has become fairly clear. These results, as well as estimates from Big Bang Nucleosynthesis [5] indicate that about 25% of the universe is composed of non-baryonic matter, which is not visible to us, while 4-5% consists of normal baryonic matter, both visible and invisible to us, and the remaining 70% of the universe is believed to be made up of a mysterious dark energy or vacuum energy which pervades space with negative pressure and causes the expansion of the universe to accelerate. Furthermore, galaxy rotation curves and x-ray measurements indicate that there is more matter in galaxies than we can see (e.g., [6,7]). Some of this "dark matter" is believed to be in baryonic form and may be located in the dark halos of galaxies (e.g., [8]). With this in mind, several experiments have been undertaken in the last 10 or so years, including the MACHO project, to carry out microlensing searches of baryonic halo dark matter in the form of such objects as brown dwarfs, white dwarfs, neutron stars, and black holes, collectively referred to as MAssive Compact Halo Objects (MACHOs).

2. Microlensing Searches for Halo Dark Matter

Here, we focus on the geometry of microlensing (Figure 1)[12] towards the LMC, a dwarf irregular galaxy in orbit around the MW, which acts as a crowded stellar background of source stars. We consider the MACHO to act as a point source point lens. If a MACHO in the halo of our galaxy passes near our line of sight to a source star in the LMC, the gravitational influence of the MACHO will cause the light from the source star to be deflected

and two distorted images on opposite sides of the lens will be produced (Figure 2)[11]. The two images will only be separated by an order of a milliarcsecond, and thus not enough to be resolved as two separate images. The source star will instead appear as a single distorted and magnified image due to the conservation of surface brightness, causing a transient increase in the source star flux which reaches the observer's eye (or telescope). The MACHO acts as a lens to the source star, and the increase in flux is known as a microlensing event. If the MACHO is exactly along the line of sight between us and the lensed source star, the image produced is that of a perfect ring with a radius known as the Einstein Ring radius, R_E , of the lens. The characteristic time scale for a microlensing event (also known as the event duration), \hat{t} , is the time it takes the source object to move with respect to the lens by one Einstein ring radius. In observing units, this is the amount of time the flux of the source star is at least 1.34 times greater than its baseline. All of the real information concerning the lensing population (mass, distance, and velocity) is contained in this observable. Given that direct measurements of the fundamental parameters (mass, velocity, and distance of the lens from the observer) are difficult to extract, the main results of microlensing surveys are expressed in terms of a quantity referred to as the 'optical depth', τ , to gravitational microlensing. Conceptually, the optical depth can be defined as the percent chance that in an observation of any single star at any given instant a microlensing event will be in progress. It is also a number equal to the sum of the durations of all microlensing events divided by the total number of stars observed times the total time of observation. Using the optical depth and the distribution of event durations one can draw conclusions about the fraction of halo dark matter which is made up of MACHOs and the most likely MACHO mass.

The MACHO collaboration observed 11.9 million stars in the LMC and found 13 to 17 events towards the LMC in 5.7 years of observations, with a most likely mass for the lenses estimated to be in the range $0.15 - 0.9 M_\odot$ assuming a standard spherical Galactic halo and derived

¹Department of Physics, University of California, Davis, CA 95616
Email: yashar@physics.ucdavis.edu

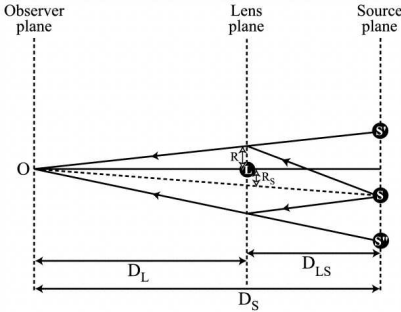


Fig. 1.— Geometry of a microlensing event. The path of a ray of light from a source object (S) is deflected by the presence of a massive lens (L), creating two images of the source at S' and S'' . The source lies a distance D_s and the lens a distance D_L from the observer (O). R_s is the impact parameter, the smallest distance between the observer-source line of sight and the lens. R is the smallest distance between the observer-image line of sight and the lens.

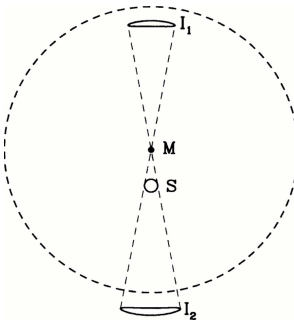


Fig. 2.— The lensing mass (M), the small circular source (S), and the two images (I_1 and I_2), are shown. In the presence of mass M the source is seen only at I_1 and I_2 and not at S. The Einstein ring is shown as a dashed circle. The radius of the circle is typically ~ 1 milliarcsecond for microlensing by MW stars.

optical depth of $\tau = 1.2 \pm 0.35 \times 10^{-7}$ [13,14]. This optical depth is too large by a factor of about 5 to be accounted for by known populations of stars. This excess is attributed to MACHOs of mass $\sim 0.5M_\odot$. Furthermore, the MACHO collaboration found a scarcity of short duration lensing events, suggesting that there is no significant population of brown dwarfs (with $M < 0.08M_\odot$) in the dark halo of the MW galaxy. The estimated mass range of $0.15 - 0.9M_\odot$ may indicate that a reasonable baryonic dark matter candidate in the MW halo could include a population of white dwarf stars.

Unpublished results from the EROS2 collaboration's microlensing survey towards the LMC [14,15] suggest that 12 - 20% of the MW halo consists of MACHOs with masses in the $2.0 \times 10^{-4} - 1M_\odot$ range, possibly compatible with the MACHO microlensing results. Furthermore, tantalizing results from two other collaborations who are conducting microlensing searches for MACHOs towards the Andromeda galaxy [16,17] suggest that at least 20-25% of the mass of Andromeda's halo is in the form of MACHOs with an average mass lying in the $0.5 - 1M_\odot$

range, similar to the MACHO collaboration's estimates for the MW halo.

3. The Location of the Microlenses

There has been a great deal of controversy over the location of the microlenses detected towards the LMC [18,19,20] since the detection of the first microlensing event [21]. Three competing explanations for the microlensing signal are that microlensing towards the LMC is caused by: (1) MACHOs in the halo of the MW, (2) the "self-lensing" of stars in the LMC by other faint stars in the LMC, and (3) a structure behind the LMC providing source stars for LMC lensing.

Three possible ways for distinguishing between a self-lensing and a halo-lensing signal, and, thus, resolving the halo-lensing or self-lensing debate, include: (1) given an agreed upon LMC model, modeling the contribution to the optical depth from known dark-matter components, subtracting this from the observed signal, and assuming that the remaining signal comes from the MW dark halo, (2) comparing the spatial distribution of the observed microlensing events with the predictions of LMC and halo models [22,23] and (3) determining the location of the lenses in some more direct fashion: those events whose lenses lie in the LMC are self-lensing and those that lie in the halo are halo-lensing.

In a standard (thin disk + bar) model of the LMC, modeling of the microlensing geometry indicates that self-lensing events are expected to make only a small contribution ($\sim 8 - 13\%$) to the total optical depth towards the LMC [18,22,23]. However, the structure and dynamics of the LMC are not completely determined, and more adventurous and creative models may (or may not) result in a significantly higher self-lensing optical depth [19,20,24,25,26,27].

Fortunately, the problem of confining the location of the lensing population can be approached in other ways. We will now explore how we can use the source star color-magnitude diagram to obtain information about the possible locations of the microlensing source stars.

4. Information from the Microlensing Source Star CMD

Here, we compare four different models for LMC microlensing. Each model involves a different microlensing geometry, in which the source stars and lenses are located in different populations. In some models, a substantial fraction of the source stars will lie *behind* the LMC disk.

The four LMC microlensing models are:

► **MW Halo-lensing:** For this model the lens is a MACHO in the MW halo and the source star is located in the LMC disk or bar. All of the source stars lie in the LMC disk and/or bar such that the source stars are representative of the average CMD of the LMC.

► **LMC Disk and/or Bar Self-lensing:** Both the lens and the source star are normal stars in the LMC disk and/or bar and, once again, none of the source stars lie behind the LMC disk and/or bar.

► **LMC Spheroid Self-lensing:** This is a reference to both LMC halo and "shroud" self-lensing. The

term "shroud" here is meant to imply an LMC population which is like a halo in that it is spatially not part of the LMC disk, but unlike a halo in that it is non-virialized and takes the form of an extended flattened spheroidal component of tidal debris [26,25]. In this model, both the lens and the source star can lie either in the LMC disk or the LMC halo. In spheroid self-lensing there are four event geometries: (1) background spheroid source and disk lens, (2) disk source and foreground spheroid lens, (3) disk source and disk lens, and (4) background spheroid source and foreground spheroid lens. We might naively expect event geometries (1) and (2) to dominate the number of expected events and so if we were to ignore the contribution to event geometries (3) and (4) we would conclude that spheroid lensing would imply that about half the source stars lie in back of or behind the LMC. However, in order to produce the total observed optical depth, the spheroid needs to be so massive that it is no longer self-consistent to ignore event geometry (4). Calculations performed in the formalism of [23] suggest instead that microlensing events with a background spheroid source and a foreground spheroid lens become an important contributor and increase the expected fraction of background source stars behind the LMC disk to ~ 0.65 .

► **Background Lensing:** In this model, introduced and pushed forward by [28,29,30], the observed microlensing events are due to "background" lensing, in which all of the source stars are located in some background population, displaced at some distance behind the LMC. Lenses for this population may then be supplied by the disk and bar of the LMC. Such a background population, however, may be nearly impossible to confirm or reject observationally, as there are nearly no limits on its size or content (provided, of course, that it is small enough to "hide" or be obscured behind the LMC.)

[31] have attempted to distinguish between these possibilities by estimating the source star locations with predictions for various LMC self-lensing and MW-lensing geometries, and, thus, locating the lenses by first locating the source stars. We have continued with this approach and attempted to improve upon it by using synthetic CMDs and a larger number of observed source stars (corresponding to 13 microlensing events).

The available self-lensing geometries are constrained by knowledge of the size, content, and structure of the LMC [13]. The most viable and quantitatively plausible models for a self-lensing population large enough to explain the total observed optical depth towards the LMC propose a thick three dimensional structure behind the LMC [29,30]. Since this population lies behind the LMC, source stars drawn from it will suffer from the internal extinction of the LMC. Additionally, since this structure may be displaced behind the LMC by some amount, source stars drawn from it should be slightly fainter and have a slightly larger distance modulus. If we find that the MACHO source stars are drawn mostly from this background population, then we can conclude that the most likely microlens population for this background source star population is the LMC itself. If the source stars are drawn mainly from the LMC, then we might conclude that the microlensing is dominated by

MW halo-lensing, since the contribution from LMC disk or bar self-lensing is known to be small [18,23].

A physically reasonable parameter for the extra reddening of the background population of source stars in our model is $E(B-V) \sim 0.13$, as inferred from the mean extinction of the LMC from [32] and corrected for galactic foreground extinction. The distance to the background population of delta distance modulus, $\Delta\mu \sim 0.3$ from the model presented by [30] is very loosely obtained by the requirement that the background (source star) population be at least transiently gravitationally bound to the LMC. We can, thus, look for evidence of background source stars by looking for evidence of extra reddening in the source star CMD. We then define f_{BKG} as the fraction of source stars which have roughly twice the average reddening of the LMC, i.e., they're on the far side of the LMC. We consider three different displacement distances, $\Delta\mu \sim 0.0$ ("model 1"), $\Delta\mu \sim 0.3$ (corresponding to ~ 7.5 kpc behind the LMC; "model 2") and $\Delta\mu \sim 0.45$ (corresponding to ~ 11.5 kpc behind the LMC; "model 3"), where we have no constraints on the size or content of the background source star population except that it must be small enough and similar enough to the LMC stellar population to have avoided direct detection.

We attempt to distinguish between source stars drawn from the average population of the LMC and source stars drawn from a population behind the LMC by examining the HST CMD of microlensing source stars and comparing it to the HST CMD of the average LMC population. From the definition of f_{BKG} , we can also distinguish between MW halo lensing and LMC disk self-lensing. These CMDs are created from WFPC2 HST photometry of MACHO microlensing source stars and their surrounding fields with care taken to identify the proper sources from severely blended ground-based MACHO images. The identification is achieved by deriving accurate centroids in the ground-based MACHO images using difference image analysis (DIA) [33] and then transforming the DIA coordinates to the HST frame. Before we can properly compare the source star CMD to the HST field CMD we must first convolve the HST field CMD with the MACHO microlensing detection efficiency as a function of stellar magnitude (see Figure 3). We choose the two-dimensional Kolmogorov-Smirnoff (KS) test [34] to quantify the probability that the observed microlensing source stars are drawn from a specific model population. The KS test results (Figure 4) indicate that the 2-D KS-test probability P is highest for $f_{BKG} \sim 0.0 - 0.2$ with very little dependence on the value of the displacement $\Delta\mu$. We rule out a model in which the source stars all belong to some background population at a confidence level of 99%. We can rule out spheroid self-lensing models ($f_{BKG} \sim 0.65$) at the statistically marginal confidence level of 80-90%. With the 13 event KS-test analysis alone, we can't exclude lensing by an LMC stellar shroud with any real significance. However, no strong observational evidence exists to support the existence of an LMC shroud, and some observational work limits the total mass of any type of spheroid to about 5% of the total mass of the LMC [35,36], which is far too small to account for the observed microlensing signal. The allowed region of the KS test result plot is consistent with the expected

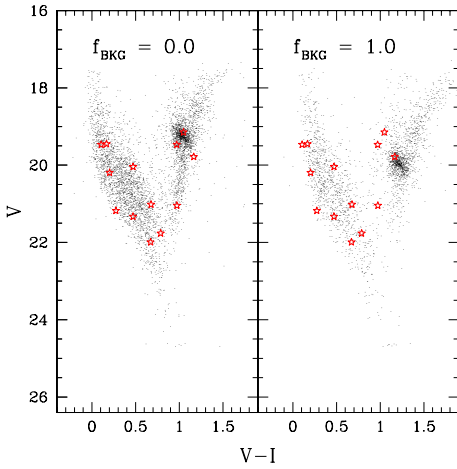


Fig. 3.— The observed MACHO microlensing source stars (large red stars), over-plotted on two model source star populations (small black dots). The left panel represents a source star population drawn entirely from the LMC disk+bar ($f_{BKG} = 0.0$). The right panel represents a model in which all of the stars belong to a background population ($f_{BKG} = 1.0$) with $\Delta\mu = 0.3$ and $\Delta E(V - I) = 0.18$.

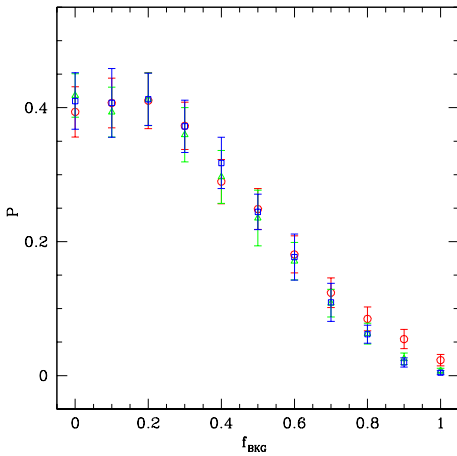


Fig. 4.— The 2-D KS test probability P that the observed distribution of source stars was drawn from a source star population in which a fraction of the source stars are located behind the LMC. The distance moduli of the background stars with $\Delta\mu = 0.0, 0.30, 0.45$ are shown as red circles, green triangles and blue squares respectively. The errors bars indicate the scatter about the mean value for 20 simulations of each model.

location of the source stars in both the MW-lensing and LMC disk+bar self-lensing geometries. However, as discussed above, detailed modeling of the LMC disk+bar self-lensing suggests that it contributes at most $\sim 13\%$ of the observed optical depth. We also note that, by definition, f_{BKG} for LMC disk-disk lensing is much higher than for MW halo lensing, indicating that the KS test results disfavor LMC disk-disk lensing. Therefore, the results of the KS test analysis presented here, taken together with

external constraints, suggest that the most likely explanation is that the lens population comes mainly from the MW halo, with a smaller self-lensing contribution from the disk and bar of the LMC. The strength of this analysis is severely limited by the number of microlensing events. Although we are currently able to exclude the most extreme model ($f_{BKG} \sim 1.0$) at a reasonable degree of confidence, more microlensing events will be necessary to more accurately determine f_{BKG} and eliminate microlensing models such as LMC "shroud" self-lensing. Ongoing microlensing surveys and projects such as SuperMACHO may provide a sufficient sample of microlensing events over the next few years. The technique outlined here could prove a powerful method for locating source stars and lenses with the use of these future data sets.

Another significant problem with the analysis outlined here, however, is that in the creation of the model source star populations, the background fraction was created from the normal, observed CMD, which already includes the background fraction and all other populations. Also, the observed CMDs we were using to create model source star populations were already reddened with the observed reddening of the LMC and foreground reddening, and reddening them again with the specified reddening model could result in too large a spread along the reddening vector. Our ongoing work involves doing a more sophisticated analysis of the MACHO source stars in relation to the general LMC population by deriving the underlying un-reddened stellar CMD and then constructing various reddening models involving uniform reddening as well as Poisson reddening models with a Poisson distribution of "cloudlets" (to make a detailed study of the effect of patchiness on the significance of the KS test) for the populations supplying the microlensing source stars, and, thus, recreating any populations we are interested in testing. We then compare these reddened model CMDs to the observed source star CMDs and the 13 microlensing source stars. The null hypothesis that we are testing is that the population of microlensing sources in the LMC came from the "normal" CMD. The alternative, is that the population of microlensing sources came from a different distribution ("background" stars). So, we are testing what model fits the observed data best, and the statistics that we use to do the testing come from the 2D KS test. It is clear that we have too few sources to make strong statements like rejecting the null hypothesis. Rather, we would like to show that the null hypothesis fits the data better than some other hypothesis (like the model in [30]). We use the synthetic CMD algorithm "StarFISH"² [37] to generate non-reddened model CMDs.

The StarFISH code package is designed to determine the best-fit star formation history (SFH) for a stellar population, given multicolor stellar photometry and a library of theoretical isochrones. The package constructs a library of synthetic CMD Hess diagrams and then uses a minimization routine to determine the linear combination of synthetic CMDs that best matches the observed photometry. When the best-fitting model is found, the

² Available from <http://marvin.as.arizona.edu/~jharris/SFH/>

amplitude coefficients modulating each synthetic CMD describe the SFH of the observed stellar population. We are then able to use the code to construct an artificial stellar population that can then be compared to the observed CMD (Figure 5). We intend to use StarFISH to produce a model CMD with a realistic reddening model that is consistent with observations.

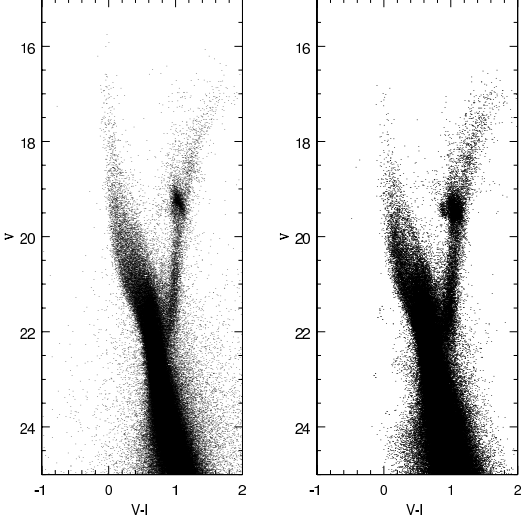


Fig. 5.— Left Panel: Observed composite HST color magnitude diagram of the 13 LMC fields surrounding each of the microlensing events. Right Panel: An example of a composite best-fit StarFISH-generated model CMD for the 13 LMC fields.

5. Future Direction of Research – Dark Energy Observables

Due to a great deal of confusion in the theoretical domain, the field of cosmic acceleration (i.e., dark energy) is highly data driven at this stage. There are a number of exciting new observational programs that could have a great impact on the field. As my own research efforts will now be transitioning into this area, I will be working on a research project with Professor Albrecht, who is now heavily involved in the question of how to define robust science goals for new observational programs to study cosmic acceleration. Much of Albrecht's current work will focus on establishing key dark energy observables that transcend the underlying theoretical uncertainties. Part of my research efforts will involve exploring the importance of different observables by investigating their utility in discriminating among a range of theoretical models, as well as comparing different methods of exploring dark energy and assessing among a number of different methods of observation. It is anticipated that some observables will have considerably more usefulness among a wide range of theoretical models, and these will make the most natural and robust observables to target and explore with new experiments. My research will also involve: (1) Learning how to use computational tools developed by Albrecht for this work, (2) expanding the tools to include new theoretical ideas which have only recently been formulated and established, (3) using these

tools to explore the space of theoretical models and determine how well a range of different observables can discriminate among them, (4) modeling observable features of dark energy onto new models of dark energy, and (5) co-authoring research publications about this work.

REFERENCES

- [1] Spergel, D.N., et al. 2003, ApJS, 148, 175
- [2] Bennett, C.L., et al. 2003, ApJS, 148, 1
- [3] Riess, A. et al. 1999, AJ, 116, 1009
- [4] Perlmutter, S., et al. 1999, ApJ, 517, 565
- [5] Tytler, et al. 2000, Phys. Rev., 333, 409
- [6] Sparke, L. & Gallagher, J. 2000, "Galaxies in the Universe - An Introduction" (Cambridge University Press)
- [7] Ryden, B. 2003, "Introduction to Cosmology" (San Francisco: Addison Wesley)
- [8] Carr, B. 1994, ARA&A, 32, 531
- [9] Refsdal, S. 1964, MNRAS, 134, 315
- [10] Paczynski, B. 1986, ApJ, 304, 1
- [11] Paczynski, B. 1996, ARA&A, 34, 419
- [12] Sahu, K. & Gilliland, R. 2003, ApJ, 584, 1042
- [13] Alcock, C., et al. 2000a, ApJ, 542, 281
- [14] Jetzer, P., et al. 2004, astro-ph/0409496
- [15] Tisserand, P. & Milsztajn, A., 2005, astro-ph/0501584
- [16] Uglesich, R., et al. 2004, ApJ, 612, 877
- [17] Novati, S.C., et al. 2005, astro-ph/0504188
- [18] Gould, A. 1995, ApJ, 441, 77
- [19] Sahu, K.S. 1994, Nature, 370, 275
- [20] Wu, X. 1994, ApJ, 435, 66
- [21] Alcock, C., et al. 1993, Nature, 365, 621
- [22] Alcock, C., et al. 1997, ApJ, 486, 697
- [23] Gyuk, G., et al. 2000, ApJ, 535, 90
- [24] Alves, D.R. & Nelson, C.A. 2000, ApJ, 542, 789
- [25] Evans, N.W. & Kerins, E. 2000, ApJ, 529, 917
- [26] Weinberg, M. 2000, ApJ, 532, 922
- [27] Zhao, H. & Evans N. 2000, ApJ, 545, 35
- [28] Zhao, H. 1999, ApJ, 527, 167
- [29] Zhao, H. 2000, ApJ, 530, 299
- [30] Zhao, H., et al. 2000, ApJ, 532, L37
- [31] Alcock, C., et al. 2001a, ApJ, 552, 582.
- [32] Harris, J., et al. 1997, AJ, 114, 1933
- [33] Tomaney, A.B., & Crotts, A.P.S. 1996, AJ, 112, 2872
- [34] Press, W.H., et al. 1992, Numerical Recipes in C, Second Edition (Cambridge: Cambridge Univ. Press)
- [35] Kinman, T.D., et al. 1991, PASP, 103, 1279
- [36] Olszewski, E.W., et al. 1996, ARA&A, 332, 1
- [37] Harris, J. & Zaritsky, D. 2001, ApJS, 136, 25